LETTER

# Cell Adhesion and Spreading Behavior on Vertically Aligned Silicon Nanowire Arrays

**Suijian Qi,[†] Changqing Yi,[†,‡] Shenglin Ji,[†] Chi-Chun Fong,[‡] and Mengsu Yang*[,†,‡]**

Department of Biology and Chemistry, City University of Hong Kong, 83 Tat Chee Avenue, Kowloon, Hong Kong SAR, China, and Key Laboratory of Biochip Technology, Biotech & Health Centre, Shenzhen Research Institute of City University of Hong Kong, Shenzhen, China

**ABSTRACT** In this report, we studied the interactions between biological cells and vertically aligned silicon nanowire (SiNW) arrays and focused on how SiNW arrays affected cellular behaviors such as cell adhesion and spreading. We observed that SiNW arrays could support cell adhesion and growth and guide cell adhesion and spreading behaviors. The results also showed that SiNW arrays could not only enhance the cell−substrate adhesion force but also restrict cell spreading. Combining the results from scanning electron microscopy images of cell morphology and the expression analysis of genes and proteins related to cell adhesion and spreading process, we proposed a mechanism on how cell adhesion and spreading was controlled by arrayed SiNWs. The effects of SiNW arrays in guiding cell adhesion and spreading behavior might be useful in the development of cell microarrays, tissue engineering scaffolds, and molecule delivery vehicles in which strong cell−substrate adhesion and reduced cell−cell communication were beneficial.

**KEYWORDS:** silicon nanowire • array • cell adhesion • cell spreading



Silicon nanowire (SiNW) has been shown to be a good candidate for applications such as field effect transistor (1), biosensor (2−5), biological material and device (6, 7), and drug delivery vehicle (8). Recently, the fabrication of vertically aligned SiNWs on a silicon wafer (hereafter referred as SiNW arrays) (9−11) has enabled the applications of SiNW in the development of electronic and photonic devices (12). The biocompatibility of silicon and the ease of control on the density, diameter, and length of arrayed SiNWs also point to biological use of a SiNW array (13). As a prerequisite, the biological effects of SiNWs as potential tissue engineering materials, molecule delivery vehicles, and cell microarray substrates need to be investigated thoroughly (13−16). In this report, we have studied the interactions between biological cells and SiNW arrays and focused on how SiNW arrays affected cellular behaviors such as cell adhesion and spreading. Cell adhesion is the first step upon interactions of material with cells and is of fundamental importance in the development and maintenance of tissues (17, 18). Here, we have characterized the cell behaviors on SiNW arrays by scanning electron microscopy (SEM), analyzed the expression levels of genes and proteins related to cell adhesion and spreading process by reverse transcription polymerase chain reaction (RT-PCR) and Western immunoblotting, and measured the cell−substrate adhesion force by a centrifugation method. The results showed that SiNW arrays could not only enhance the cell−substrate adhesion force but also restrict cell spreading. A mechanism was proposed on how cell adhesion and spreading were controlled by arrayed SiNWs.

* Author to whom any correspondence should be addressed. E-mail: bhmyang@cityu.edu.hk.
Received for review August 28, 2008 and accepted October 29, 2008
[†] City University of Hong Kong.
[‡] Shenzhen Research Institute of City University of Hong Kong.
DOI: 10.1021/am800027d


## RESULTS AND DISCUSSION

The study on cell adhesion and spreading behavior was carried out on SiNW arrays fabricated by self-assembling nanoelectrochemistry with some modifications on the literature process (8). As shown in Figure 1, SiNWs were vertically aligned on the silicon wafer, with the wires having diameters of about 100 nm, lengths of about 20 $\mu$m, and tens of wires bundled together forming flower-like structures (Figure 1A,B). The morphological images of cells incubated on SiNW arrays and on a flat silicon wafer were characterized by SEM, as shown in Figure 1C−H. Most LX-2 and HepG2 cells were seen attaching to the top of the SiNW array (Figure 1E,F), with the cell filopodia grasping the SiNWs underneath and around (Figure 1G,H). No cell was seen attaching to the side of SiNW or at the bottom of the array. The spreading profile of the cells on the SiNW array was different from that on the flat silicon wafer (Figure 1C,D); the cells on the SiNW array did not stretch out as freely as those on a flat silicon wafer, therefore they had relatively smaller cell sizes.

The viability of cells incubated on the SiNW array and the flat silicon wafer for 18 and 48 h was evaluated using an Alamar Blue assay (19). LX-2 and HepG2 cells were viable after they were incubated on the SiNW array for 18 and 48 h, respectively, and their viabilities were greater than 92% (see Table 1), indicating that the SiNW array showed biocompatibility similar to that of other nanowire structures (20, 21).

The cells adhered on the SiNW array and on the flat silicon wafer were harvested with trypsin−ethylenediaminetetraacetic acid (EDTA), and the adhered cell number per square millimeter was counted. Both LX-2 and HepG2 cells


Published on Web 11/24/2008

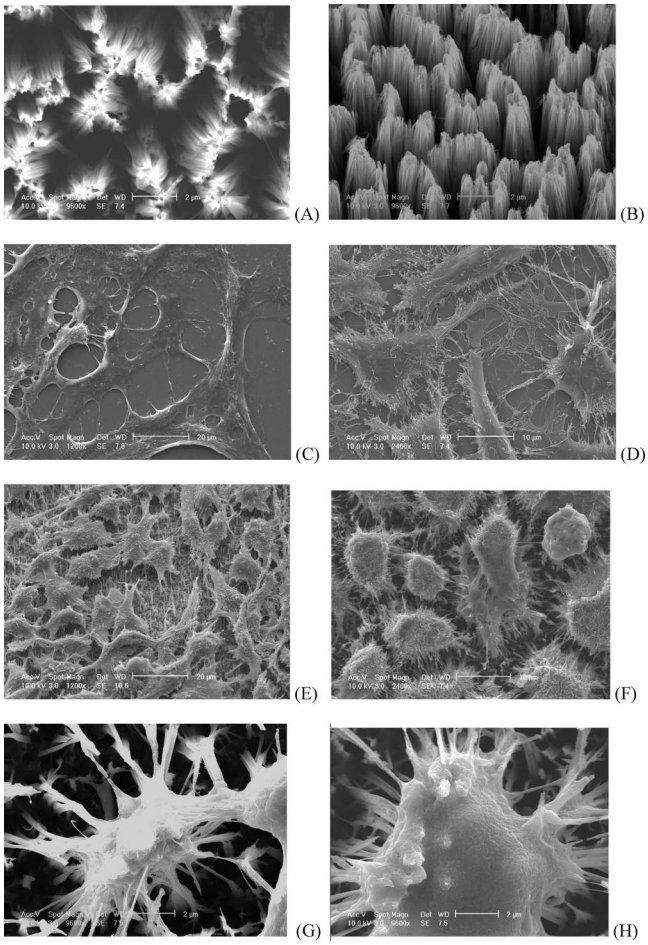

FIGURE 1. SEM images of the fabricated SiNW arrays and the cells cultured on silicon substrates: (A) top view of the SiNW array; (B) 30° tilt view of the SiNW array; (C) LX-2 cells on a flat silicon wafer; (D) HepG2 cells on a flat silicon wafer; (E) LX-2 cells on a SiNW array; (F) HepG2 cells on a SiNW array; (G) view in which the filopodia of LX-2 cells were reaching out for the SiNWs underneath and around; (H) view in which the filopodia of HepG2 cells were reaching out for the SiNWs underneath and around.

**Table 1. Relative Cellular Viability (%) on a SiNW Array and on a Silicon Wafer[a]**

| incubation time | 18 h | 48 h |
|---|---|---|
| HepG2 cell on a flat silicon wafer | 103 ± 7 | 105 ± 12 |
| HepG2 cell on a SiNW array | 92 ± 15 | 100 ± 17 |
| LX-2 cell on a flat silicon wafer | 100 ± 13 | 102 ± 11 |
| LX-2 cell on a SiNW array | 93 ± 18 | 96 ± 12 |

[a] Data are shown as the mean ± standard errors of three independent experiments.

had slightly lower counts on the SiNW array than on the flat silicon wafer after 4, 18, and 48 h of incubation (see Table 2).

As the cells were grasping as many as SiNW underneath and around with their filopodia, we hypothesized that the adhesion force between cells and SiNW array may be stronger than that between cells and silicon wafer. To verify this, we carried out experiments to test the adhesion force between the cells and substrates using a centrifugation method. We also attempted to use atomic force microscopy (AFM) to detect the cell−substrate adhesion force. However,

**Table 2. Adhered Cell Number per Square Millimeter on a SiNW Array and on a Silicon Wafer after Cells Were Harvested with Trypsin−EDTA[a]**

| incubation time | 4 h | 18 h | 48 h |
|---|---|---|---|
| HepG2 cell on a flat silicon wafer | 100 ± 2 | 101 ± 3 | 99 ± 2 |
| HepG2 cell on a SiNW array | 91 ± 5 | 102 ± 4 | 88 ± 6 |
| LX-2 cell on a flat silicon wafer | 96 ± 7 | 100 ± 4 | 100 ± 5 |
| LX-2 cell on a SiNW array | 88 ± 8 | 92 ± 1 | 90 ± 6 |

[a] Data are shown as the mean ± standard errors of three independent experiments.

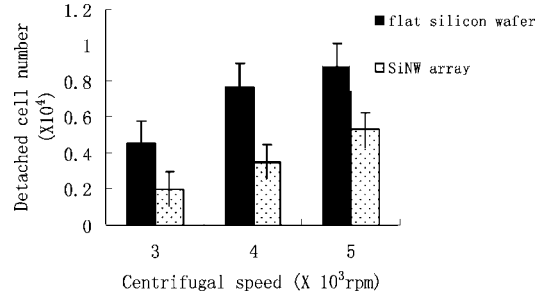


FIGURE 2. Relationship between the detached cell number and the centrifugal speed. After HepG2 cells were adherent to the substrates (flat silicon wafer and SiNW array), centrifugal forces were applied to detach the cells from the substrates. Under the same centrifugal forces, more cells detached from the flat silicon wafer than from the SiNW array. Data are shown as the mean ± standard errors of three independent experiments.

in our case, AFM is not a suitable tool to detect the cell−SiNW array adhesion force because of the deep pits (about 20 $\mu$m deep) in the SiNW array (see Figure 1B). The tip of the atomic force microscope was always stuck in the pits and could not work properly. As an alternative, the centrifugation method could provide information on the cell−substrate adhesion force, although it could not measure the adhesion force values directly. The results showed that, with the same number of cells seeded on the substrates, under the same centrifugal force more cells were detached from the flat silicon wafer than from the SiNW array (see Figure 2), which suggested that the adhesion force between the cells and the SiNW array was greater than that between the cells and the flat silicon wafer.

To further understand the molecular basis of how SiNW arrays affect cell adhesion and spreading behavior, the expression levels of several genes known to be related to the cell adhesion process and cellular components such as the extracellular matrix and cytoskeleton, including integrin, focal adhesion kinase (FAK), type I collagen (Col I), and α-actin, were analyzed by RT-PCR. The results showed that the expression levels of Col I and α-actin were down-regulated after HepG2 cells were incubated on the SiNW arrays for 18 and 48 h, which may account for the restricted spreading behavior of cells on the SiNW array. On the other hand, the expression levels of integrin and FAK were both up-regulated, which may explain the enhancement of cell adhesion on the SiNW array (see Figure 3).

The protein expression levels of α-actin and type I collagen were further examined by Western immunoblotting. The results showed that the expression levels of α-actin and

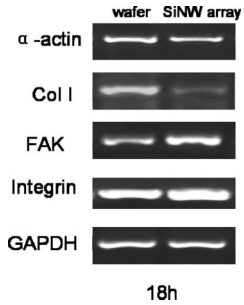


FIGURE 3. Gel electrophoresis (1.5% agarose) images showing RT-PCR results of adhesion-specific genes. The GAPDH gene was used as the endogenous reference house-keeping gene.

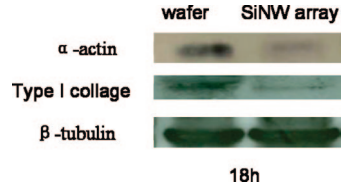


FIGURE 4. Western immunoblotting results of α-actin and type I collagen in HepG2 cells cultured for 18 h on the flat silicon wafer and the SiNW array. β-Tubulin was used as an endogenous reference.

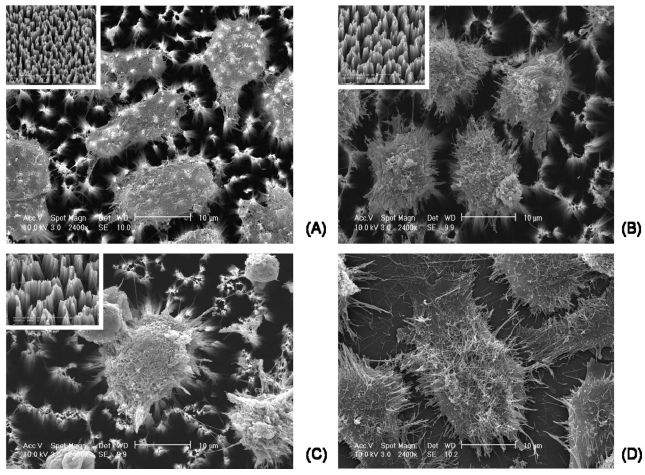


FIGURE 5. SEM images of HepG2 cells cultured on different patterns of SiNW arrays and on the flat silicon wafer: (A) cells on the SiNW array with a high density of nanowires; (B) cells on the SiNW array with a medium density of nanowires; (C) cells on the SiNW array with a low density of nanowires; (D) cells on the flat silicon wafer. Each inset in A–C represents the 30° tilt view of the SiNW array.

type I collagen were both down-regulated after HepG2 cells were cultured on the SiNW array for 18 h compared with those cultured on the flat silicon wafer (see Figure 4), consistent with RT-PCR results.

In order to determine whether the above-observed effects on the cell–SiNW array interaction were due to an increase in the surface area or the specific nanostructure features, SiNW arrays with different patterns of nanowires were fabricated. The arrays were classified as high density (H; the interval between neighboring silicon clusters is about 1 μm), medium density (M; the interval between neighboring silicon clusters is about 2 μm), or low density (L; the interval between neighboring silicon clusters is about 3 μm) with regard to their nanowire patterns. These arrays shared the common property that there were nanostructured features

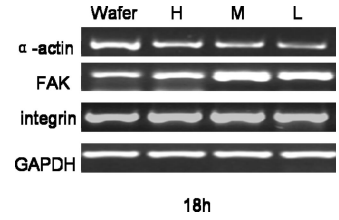


FIGURE 6. Gel electrophoresis (1.5% agarose) images showing RT-PCR results of α-actin, FAK, and integrin genes. The GAPDH gene was used as the endogenous reference house-keeping gene.

on the surfaces but with different surface areas. The results described above were all carried out using the high-density SiNW arrays. We have further carried out following preliminary study to show that cells were able to adhere to all of the arrays with different densities with similar behaviors, where less spreading (smaller cell size) was observed when compared with those on the flat silicon wafer (see Figure 5). The observation suggested that it was the presence of the nanostructured features that caused the enhanced cell adhesion rather than the changes in the surface areas.

The gene expression levels of α-actin, integrin, and FAK of HepG2 cells on different SiNW arrays (H, M, and L) were also evaluated (see Figure 6). The expression levels of α-actin on H, M, and L SiNW arrays were all down-regulated compared with that on the flat silicon wafer, consistent with SEM characterization that cells on the arrays had less spreading cytoskeletons. The expression levels of integrin and FAK on SiNW arrays were all up-regulated compared with that on the flat silicon wafer. The significantly enhanced expressions of FAK on the SiNW arrays were more likely due to the needlelike nanostructures of the arrays rather than the surface area change because the expression of FAK was independent to the different surface areas of SiNW arrays.

On the basis of these results, we proposed a mechanism on how arrayed SiNWs might influence cell adhesion and spreading. When cells first come into contact with the SiNW arrays, the nonflat and needlelike nanostructures stimulate the cells to extend more filopodia to form focal adhesion points with the substrate, reaching out to as many SiNWs around and underneath as possible. Therefore, the expression of FAK was obviously up-regulated at the early stage of cell adhesion. At the same time, the relatively large interval space between every cluster of SiNWs makes it impossible for the cells to reach out for the SiNWs at a distance from their first contact point. Consequently, further spreading of the cell skeleton is restricted as reflected by the down-regulation of the α-actin expression.

In conclusion, our results showed that the SiNW arrays exhibited good biocompatibility with biological cells and could support and favor cell adhesion. The SiNW arrays influenced cell adhesion and spreading in two aspects: enhancing the cell–substrate focal adhesion force and restricting cell spreading. The effects of SiNW arrays in guiding cell adhesion and spreading behavior might be useful in the development of cell microarrays, tissue engineering scaffolds, and molecule delivery vehicles in which strong

cell–substrate adhesion and reduced cell–cell communication were beneficial.

## METHODS

**Fabrication of SiNW Arrays.** SiNW arrays were fabricated by self-assembling nanoelectrochemistry (8), with some modifications on the process. In brief, the synthesis reaction was conducted in a sealed Teflon container. A P(100) silicon wafer (cut into 0.7 cm × 0.7 cm pieces so that the fabricated samples would fit into the well of cell culture plates) was degreased with acetone and ethanol, and then silver nanoparticles were electroplated onto the cleaned silicon surface by immersing the wafer into a solution that contained 4.6 M HF and 0.01 M $AgNO_3$. The silver-deposited silicon wafer was then etched for 30 min in an etching solution that contained 4.6 M HF and 0.1 M $H_2O_2$. Then, the thick silver dendrite wrapping the sample was removed by treating the sample with concentrated $HNO_3$. The obtained sample was rinsed thoroughly with deionized water and dried at room temperature. The sample was examined using SEM (FEI/Phillips XL 30 ESEM-FEG). Different patterns of SiNWs on the arrays were obtained by controlling the concentration of $H_2O_2$ in the etching solution. A high density of the SiNWs pattern (H) was obtained using 4.6 M HF and 0.075 M $H_2O_2$, a medium density of the SiNWs pattern (M) was obtained using 4.6 M HF and 0.1 M $H_2O_2$, and a low density of the SiNWs pattern (L) was obtained using 4.6 M HF and 0.125 M $H_2O_2$.

**Cell Culture.** Immortalized human hepatic cell line (HSC) LX-2 was provided by Dr. Alex Hui of the Division of Gastroenterology and Hepatology, Department of Medicine and Therapeutics, Prince of Wales Hospital, Hong Kong. Cells were cultured with Dulbecco's modified eagle medium supplemented with 10% fetal bovine serum (FBS), 2 mM L-glutamine, and 1% penicillin and streptomycin at 37 °C in a humidified 5% $CO_2$ incubator. HepG2 (human hepatoma cell line) was obtained from American type Culture Collection (Manassas, VA). Cells were cultured in a RPMI 1640 medium supplemented with 10% FBS, 1% L-glutamine, penicillin, and streptomycin at 37 °C in a humidified 5% $CO_2$ incubator.

**In Vitro Cell Culture Assays.** Before all of the cell experiments, the SiNW array and silicon wafer were soaked in 70% ethanol and then UV irradiation to sterilize. The cell viability was evaluated by an Alamar Blue assay: In a 96-well polystyrene cell culture plate with square wells (0.7 cm × 0.7 cm; Seahorse Labware, Chicopee, MA), $1 \times 10^4$ cells were seeded in each well with the SiNW array or silicon wafer at the bottom of the wells and then incubated for 18 and 48 h at 37 °C in a humidified 5% $CO_2$ incubator, respectively. Cells seeded in the wells of the polystyrene plate were used as controls, and wells without cells were used as blanks. At the conclusion of the treatment, the medium was removed and the cells were washed with phosphate-buffered saline (PBS) once, and then an Alamar Blue (Sigma) solution (2 mg/mL in a cell culture medium, 200 μL) was added to each well and incubated for another 4 h at 37 °C in a humidified 5% $CO_2$ incubator. Fluorescence was read in a microplate reader (530 nm excitation and 584 nm emission). The relative viability was expressed as a percentage of $[OD_{sample} - OD_{blank}]/[OD_{control} - OD_{blank}]$. Each experiment was performed in triplicate.

**Morphological Observation.** The morphologies of HepG2 and LX-2 cells during adhesion on the SiNW array or on the flat silicon wafer after 4, 18, and 48 h of culture were observed by SEM. The cell density was $1 \times 10^4$ cells/mL. At the conclusion of the incubation, cells were washed with PBS and 0.1 M cacodylate buffer and then fixed in a fixative (2% glutaradelyde + 2% paraformaldehyde) in a 0.1 M cacodylate buffer, pH 7.8, for 2 h at 4 °C and postfixed with 1% osmium tetroxide for 1 h at room temperature. Fixed samples were washed twice with PBS, dehydrated through a graded ethanol series, and then soaked twice in hexamethyldisilazane for 1 min. Dried samples were sputter-coated with gold–palladium and examined with SEM (FEI/Phillips XL 30 ESEM-FEG) at a 5 kV accelerating voltage.

**Adhesion Force Measurement.** A total of $1 \times 10^4$ cells were seeded on the SiNW array or silicon wafer for 18 h. Then the substrate (SiNW array or silicon wafer) with attached cells was placed upside down (with cells facing down) in a centrifugal tube. The tube was filled with a cell culture medium to merge the back of the substrate. A $3 \times 10^3$ rpm ($0.7 \times 10^3 g$ force) to $5 \times 10^3$ rpm ($2 \times 10^3 g$ force) centrifugal effect was applied to the tube, and the number of cells detached from the substrate were counted.

**Adhesion-Specific Gene Expression Profile.** HepG2 cells were seeded on the SiNW array for 18 and 48 h, respectively (cells seeded on the silicon wafer were used as controls). Total RNA was extracted using TRI Reagent (Molecular Research Center, Inc., Cincinnati, OH) according to the manufacturer's instruction. Total RNA was quantified by a biophotometer (Eppendorf, Hamburg, Germany), and the quality of total RNA was checked based on the 28S/18S rRNA ratio after agarose gel electrophoresis. A total of 2 μg of each total RNA sample was used for reverse transcription under standard conditions. The resulting cDNA was used as the template in subsequent PCR. Sequences of interest were amplified using the following primer pairs: α-actin (5′-ATC TGG CAC CAC ACC TTC TA-3′, 5′-AGC TCG TAG CTC TTC TCC AG), integrin (5′-GAC CTG CCT TGG TGT CTG TGC-3′, 5′- AGC AAC CAC ACC AGC TAC AAT-3′), FAK (5′-GAA GTC TTC AGG GTC CGA TTG-3′, 5′- CAT TCT CGT ACA CCT TAT CAT TCG-3′), type I collagen (5′-AAC ATG ACC AAA AAC CAA AAG TG-3′, 5′-CAT TGT TTC CTG TGT CTT CTG G-3′). GAPDH (5′-GAC TTC AAC AGC AAC TCC CAC-3′, 5′-TCC ACC ACC CTG TTG CTG TA-3′) was used as endogenous reference housekeeping genes.

**Western Immunoblotting.** Western immunoblotting of type I collage and α-actin was performed after 18 h of culture. Proteins were collected in distilled water supplemented with 1% (v/v) Triton X-100, 50 mM Tris–HCl, 10 mM EDTA, and 26% (w/v) urea. Proteins were fractionated by electrophoresis and electrotransferred to a nitrocellulose membrane (Amersham Biosciences, Piscataway, NJ). After blocking with 5% (w/v) bovine serum albumin solution in

TBST [10 mM Tris, 150 mM NaCl, and 0.05% (v/v) Tween 20], the blots were exposed to mouse antibodies specific to type I collage (CalBioChem, CP17L) and α-a ctin (DakoCytomation M 0851). After a reaction with secondary antibody, immunoreactive bands were visualized using enhanced chemiluminescence detection and quantified using Quality One software (Bio-Rad). Blots were stripped and reprobed for the loading control of β-tubulin (Santa Cruz, 9104).

**Acknowledgment.** This work was supported by the Central Allocation Grant Scheme of the Research Grants Council of Hong Kong SAR, China (City U 3/04 C), City University of Hong Kong (Project 7002100), and Key Laboratory Fund of Shenzhen Municipal Government, China.

## REFERENCES AND NOTES

(1) Duan, X. F.; Niu, C. M.; Sahi, V.; Chen, J.; Parce, J. W.; Empedocles, S.; Goldman, J. L. *Nature* **2003**, *425*, 274–278.
(2) Streifer, J. A.; Kim, H.; Nichols, B. M.; Hamers, R. J. *Nanotechnology* **2005**, *16*, 1868–1873.
(3) Patolsky, F.; Timko, B. P.; Yu, G. H.; Fang, Y.; Greytak, A. B.; Zheng, G. F.; Lieber, C. M. *Science* **2006**, *313*, 1100–1104.
(4) Chen, W. W.; Yao, H.; Zhu, J. J.; Yang, M. S.; Lee, S. T. *Appl. Phys. Lett.* **2006**, *88*, 213104.
(5) Gao, Z. Q.; Agarwal, A.; Trigg, A. D.; Singh, N.; Fang, C.; Tung, C. H.; Fan, Y.; Buddharaju, K. D.; Kong, J. M. *Anal. Chem.* **2007**, *79*, 3291–3297.
(6) Li, Z.; Chen, Y.; Li, X.; Kamins, I.; Nauka, K.; Williams, R. S. *Nano Lett.* **2004**, *4*, 245–247.
(7) Shao, M. W.; Shan, Y. Y.; Wong, N. B.; Lee, S. T. *Adv. Funct. Mater.* **2005**, *15*, 1478–1482.
(8) Kwon, N. H.; Beaux, M. F.; Ebert, C.; Wang, L. D.; Lassiter, B. E.; Park, Y. H.; Mcllroy, D. N.; Hovde, C. J.; Bohach, G. A. *Nano Lett.* **2007**, *7*, 2718–2723.
(9) Peng, K. Q.; Yan, Y. J.; Gao, S. P.; Zhu, J. *Adv. Mater.* **2002**, *14*, 1164–1167.
(10) Peng, K. Q.; Yan, Y. J.; Gao, S. P.; Zhu, J. *Adv. Funct. Mater.* **2003**, *13*, 127–132.
(11) Qiu, T.; Wu, X. L.; Yang, X.; Huang, G. S.; Zhang, Z. Y. *Appl. Phys. Lett.* **2004**, *84*, 3867–3869.
(12) Wang, Q.; Li, J. J.; Ma, Y. J.; Bai, X. D.; Wang, Z. L.; Xu, P.; Shi, C. Y.; Quan, B. G.; Yue, S. L.; Gu, C. Z. *Nanotechnology* **2005**, *16*, 2919–2922.
(13) Kim, W.; Ng, J. K.; Kunitake, M. E.; Conklin, B. R.; Yang, P. D. *J. Am. Chem. Soc.* **2007**, *129*, 7228–7229.
(14) Nagesha, D. K.; Whitehead, M. A.; Coffer, J. L. *Adv. Mater.* **2005**, *17*, 921–924.
(15) Popat, K. C.; Daniels, R. H.; Dubrow, R. S.; Hardev, V.; Desai, T. A. *J. Orthop. Res.* **2006**, 619–627.
(16) Qi, S. J.; Yi, C. Q.; Chen, W. W.; Fong, C. C.; Lee, S. T.; Yang, M. S. *ChemBioChem* **2007**, *8*, 1115–1118.
(17) Hansen, L. K.; Mooner, D. J.; Vacanti, J. P.; Ingber, D. E. *Mol. Biol. Cell* **1994**, *5*, 967–975.
(18) Ben-Ze'ev, A.; Shtutman, M.; Zhurinsky, J. *Exp. Cell Res.* **2000**, *261*, 75–82.
(19) O'Brien, J.; Wilson, I.; Orton, T.; Pognan, F. *Eur. J. Biochem.* **2000**, *267*, 5421–5426.
(20) Hallstrom, W.; Martensson, T.; Prinz, C.; Gustavsson, P.; Montelius, L.; Samuelson, L.; Kanje, M. *Nano Lett.* **2007**, *7*, 2960–2965.
(21) Prinz, C.; Hallstrom, W.; Martensson, T.; Samuelson, L.; Montelius, L.; Kanje, M. *Nanotechnology* **2008**, *19*, 345101.

AM800027D